

Laboratory Evaluation of Tundish Covering Powders and Rice Hull Ash on Cleanliness for a SAE 1055 Modified Steel

Felipe Buboltz Ferreira^{a*} , Jeferson Leandro Klug^b , Julio Anibal Morales Pereira^a,
Wagner Viana Bielefeld^a, Antônio Cezar Faria Vilela^a

^aUniversidade Federal do Rio Grande do Sul, Departamento de Metalurgia,
Laboratório de Siderurgia, Av. Bento Gonçalves 9500, 91501-970, Porto Alegre, RS, Brasil.

^bUniversidade Federal do Ceará, Departamento de Engenharia Metalúrgica e de Materiais, Campus do Pici, 729, 60444-554, Fortaleza, CE, Brasil.

Received: April 28, 2022; Revised: January 26, 2023; Accepted: February 01, 2023

The continuous casting tundish is the last metallurgical reactor where molten metal flows before solidifying in the continuous casting mold. A tundish covering powder can be used for improving steel cleanliness; in this case it is named 'active tundish slag'. The objective of this work is to evaluate, in laboratory, the effect of three kinds of tundish covering powders on cleanliness for a SAE 1055 modified steel - a Ca-aluminate, a Ca-Mg-aluminate, and an Al-silicate powder, analysing their interaction with rice hull ash. The forementioned materials were molten on liquid steel, representing different kinds of tundish covering powders which are used in the steel industry: a Ca-Mg-aluminate, an Al-silicate, and a Ca-aluminate. Experiments were performed with and without a top layer of rice hull ash, simulating industrial conditions. Distribution, density, and mean diameter of inclusions were measured through automated inclusion analyses. Through computational thermodynamics it was possible to evaluate deviation from saturation (considering Al_2O_3 and MgO from refractory) and slag viscosity. It can be stated that the Ca-aluminate tundish covering powder gives better results regarding cleanliness for the SAE 1055 modified steel under laboratory conditions.

Keywords: *tundish covering materials, tundish slag, non-metallic inclusions, automated inclusion analysis, computational thermodynamics.*

1. Introduction

In the continuous casting machine, a tundish is a reservoir and distributor for liquid steel from the ladle into the molds. Tundish covering powders have the following key functions: (i) thermal insulation to minimize heat loss from steel surface, (ii) reoxidation prevention by the atmosphere and (iii) absorption of non-metallic inclusions¹⁻⁷.

Regarding the first key function - thermal insulation, retaining heat within the tundish is important for controlling the superheating level and to avoid skulling. Low bulk density and high melting temperature are the primary factors determining insulating capability. Rice husk ash is typically used since it has good thermal insulation properties; on the other hand, when only using rice hulk ash there is no hermetic sealing of the steel against air since there is no liquid slag, and of course no absorption of non-metallic inclusions. In addition to rice husk ash, it is necessary to add another material to get the metallurgical function⁸. Great diversity of tundish covering materials are used in the steel industry, differentiated by chemical and physical properties. Acid aluminum silicate types are commonly used, but they have the potential of reacting with steel and often possess a quite limited capacity to dissolve alumina or spinel type

inclusions. Basic Ca-(Mg-) aluminate type slags have the potential for wide use since they are chemically stable and have sufficient capacity to absorb inclusions³.

The three key functions of a tundish covering powder can be fulfilled when combining rice husk ash with a low melting point slag, such as Ca-aluminate, providing reoxidation prevention by the atmosphere and absorption of inclusions; however, they are poor insulators, and because of that, it is necessary to use rice husk ash on top. This combination of materials is recommended to produce low sulfide steels since calcium aluminate slag presents good sulfide capacity, which changes a bit in case of entrapped ladle slag⁹. Moreover, it has been shown through dissolution investigations using Confocal Laser Scanning Microscope, that Al_2O_3 and MgO. Al_2O_3 spinel present high dissolution rates in Ca-aluminate slag³.

When using a metallurgically active tundish slag, it is possible to promote inclusion removal from liquid steel and to prevent appearance of new and often macroscopic inclusions. With a computerized construction of phase diagrams, it is possible to compare different slags and to find proper slag compositions with reasonable capacity to dissolve inclusions, considering deviation from saturation as a parameter³.

*e-mail: felipebuboltz@gmail.com

The main objective of this work was to investigate, in laboratory, the influence of three kinds of tundish covering powders and of rice hull ash on cleanliness for a SAE 1055 modified steel - a Ca-aluminate, a Ca-Mg-aluminate, and an Al-silicate powder. Therefore, inclusion analysis was performed for steel samples after interaction with the covering materials and refractory at 1540 °C during 30 min. Furthermore, the chemical interactions which occurred among the steel, slag and refractory during the tests were analysed.

2. Materials and Methods

For the experimental work, different combinations of materials were heated in MgO crucibles at 1540 °C, according to Table 1. The powders were named as CM1 (Ca-Mg-aluminate slag), CM2 (Al-silicate slag) and CM3 (Ca-aluminate slag). RHA is rice hull ash.

Table 1 shows combinations of materials which were melted for the experimental work. Each heat was done twice, so twelve experiments were carried out.

After the heats, steel samples were collected from crucible and cut as illustrated at Figure 1. The highlighted area (crosshatched) was used for automated analysis of nonmetallic inclusions, using an ASPEX apparatus, which is an automated scanning electron microscope equipped with energy-dispersive spectroscopy. Analyzed area was 100 mm² per steel sample. Then inclusion distribution, density and mean diameter were determined. Slag samples for CM1 and CM3 were also collected (after the runs).

Table 2 shows steel composition. This steel is applied in the automotive industry as a wheel hub. Elemental composition was determined with an Optical Emission Thermo model ARL 4460 and with LECO TC-436 for total oxygen (T.O.). It was deoxidized with Si and Mn.

Compositions of tundish covering powders and of rice hull ash, determined with X-Ray Emission Spectrometer Philips model PW-2600, are at Table 3.

Steel and covering materials were melted at 1540 °C with a plateau time of 30 minutes, in MgO crucibles, with 64 mm internal diameter, 72 mm external diameter and 103 mm

Table 1. Combinations of materials, melted for the experimental work.

Heat	Steel	CM1	CM2	CM3	RHA
1	X	X			
2	X	X			X
3	X		X		
4	X		X		X
5	X			X	
6	X			X	X

Table 2. Chemical composition of the SAE 1055 modified steel which was used for the experimental work, in wt% (as-received industrial sample).

C	Si	Mn	P	S	Cr	Ni	Cu	Al	Mo	T.O. ^{a)}
0.57	0.27	0.87	0.01	0.005	0.22	0.02	0.03	0.005	0.01	3.66

^{a)} ppm

Table 3. Elemental compositions of the tundish covering powders and of the rice hull ash, in wt.% (as-received industrial samples).

Materials	%CaO	%SiO ₂	%Al ₂ O ₃	%MgO	%FeO	%TiO ₂
CM1	55.7	5.3	20.7	17.2	1.0	0.1
CM2	2.1	63.8	26.7	2.0	4.2	1.2
CM3	48.4	0.7	48.6	1.8	0.5	0.1
RHA	0.7	97.4	0.1	1.8	0.0	0.0

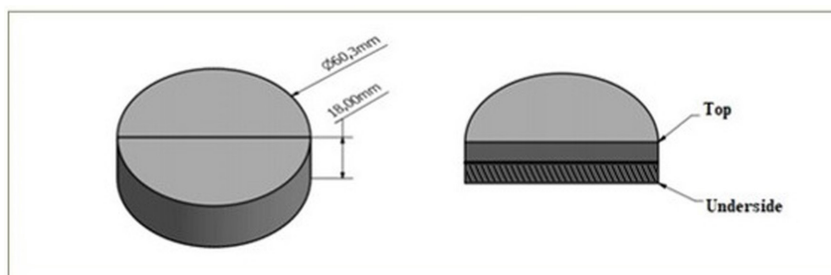


Figure 1. Representation of the area analyzed in each sample. The crosshatched area (underside) was used for automated analysis of nonmetallic inclusions.

height. The experiments were carried out in a resistive furnace ‘HT-2100-Spezial’; details on this apparatus can be found in¹⁰. The furnace works with a constant flux of argon (82 liters per hour) to avoid reoxidation by air.

Thermodynamic calculations were done with the commercial software FactSage v. 7.3 using equilibrium module¹¹. The *FToxid*, *FactPS*, *FTmisc* databases were used in the simulation. The compositions of the inclusions were represented in ternary diagrams using a program developed in Microsoft Excel¹¹. Regarding dissolution of alumina inclusions, the thermodynamic alumina driving force ΔC was calculated as shown in Equation 1.

$$\Delta C = (Al_2O_3)_{sat} - (Al_2O_3)_{bulk} \quad (1)$$

where $(Al_2O_3)_{bulk}$ is the alumina content in the slag liquid fraction, and $(Al_2O_3)_{sat}$ is the alumina saturation point.

The liquid slag viscosity η was calculated with the *Viscosity* module with the *Melts* database. Roscoe-Einstein’s equation¹² was used to calculate effective viscosity η_e through Equation 2.

$$\eta_e = \eta(1-c)^{-2.5} \quad (2)$$

Where c is the solid fraction.

3. Results and Discussion

3.1. Inclusion analysis

Table 4 shows inclusion density per type of the quantified parameters of the inclusions experimental results for the as-received industrial steel sample and for the steel samples taken after the heats. In this classification, inclusions are divided in Ca-aluminate, spinel, MgO, CaS, Ti, Al_2O_3 and Oxides. ‘Oxides’ means oxides of Mg, Al, Si, Ca and Mn, with variable composition.

It is noteworthy that inclusion density and mean diameter tends to increase, when considering the as-received industrial steel sample used as a benchmark. This happens because the laboratory conditions are different from the dynamic

industrial conditions, since the materials were confined in the MgO crucible during 30 minutes at 1540 °C. Therefore, there was more time for interactions among steel, slag and refractory, when comparing with industrial conditions. In this way, it is possible to evaluate which arrangement is less harmful for the steel cleanliness.

For the as-received steel industrial sample - used here as benchmark, there are about two inclusions per square millimeter; most of them are of the spinel type (Table 4).

Figure 2 shows inclusion density by range of size, for all the experiments conducted in this work.

The worst result, when considering inclusion density for the size $> 15 \mu m$ and comparing with the benchmark, is related to the Ca-Mg-aluminate slag CM1 (Heat 1 and Heat 2), according to Figure 2. Inclusion density for these bigger inclusions is much higher for the arrangements with the Ca-Mg-aluminate slag (CM1) than for the others (Al-silicate slag and Ca-aluminate slag, CM2 and CM3 respectively).

For CM2 and CM3 - with or without RHA -, some bigger inclusions ($> 15 \mu m$) were detected, but with lower density. Besides, there is a tendency of increasing in density for the smaller inclusions, between the range (0.5 to 5) and (2.5 to 15) μm .

Figure 3 shows in the ternary diagram the distribution of compositions of inclusions by size in the system CaO- Al_2O_3 -MgO, for both tests of Heat 6 with (steel+CM3+RHA) comparing with the benchmark. From the ternary diagram it is observed that for the benchmark steel sample, (Figure 3a), all of the inclusion diameter ranges are located in the spinel region, with few smaller diameter inclusions in the liquid region (low melting point calcium aluminates region). Next, (Figure 3b), composition of inclusions in the spinel region is still observed, however, with low densities for inclusions with smaller diameters. Finally, (Figure 3c), compositions of dispersed inclusions of various diameters in the MgO region (periclase) in the smaller ranges (0.5-2.5); (2.5-5) with inclusion compositions in the range of (5-15) and (>15) μm in the liquid region.

Figure 3b and c shows on ternary diagrams that inclusions $> 15 \mu m$ have composition on the area of liquid calcium aluminate. This composition is similar to CM3 material. This indicates an exogenous origin for these big inclusions.

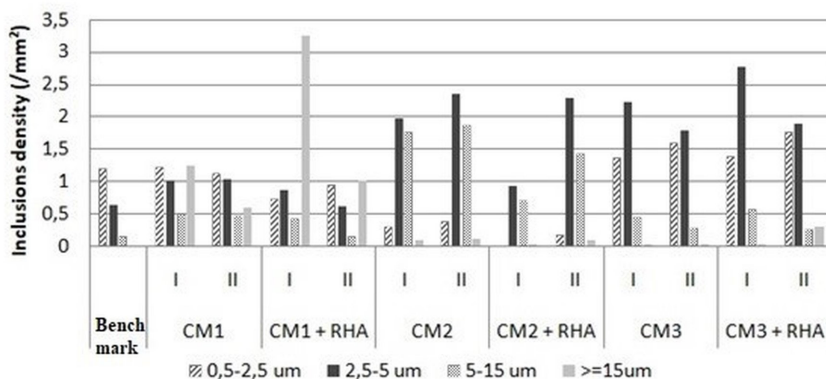


Figure 2. Inclusion density by range of size, for all the experiments conducted in this work.

Table 4. Summary of the experimental results of the samples by density per type (/mm³), composition and diameter of inclusions (µm) in the samples.

Steel sample (benchmark)	Test	Inclusion Density	Ca-aluminate	MgO·Al ₂ O ₃ (spinel)	MgO	CaS	Ti	Al ₂ O ₃	Oxides	Non Classified	Mean diameter	Standard deviation
	-	2.00	0.02	1.61	0	0	0.04	0	0.33	0	2.75	1.42
Heat 1 steel + CM1	I	3.97	0.17	0	1.26	0.20	0.04	0.02	2.28	0	23.34	35.14
	II	3.20	0.08	0	1.24	0.11	0	0.02	1.75	0	8.92	11.82
Heat 2 steel + CM1 + RHA	I	5.27	0.05	0.01	0.95	0.06	0.04	0.01	4.14	0.01	38.90	35.21
	II	2.73	0.02	0	0.94	0.13	0.02	0.01	1.61	0	21.15	27.11
Heat 3 steel + CM2	I	4.15	0.01	1.70	0.10	0.01	0	0.01	0.80	1.52	6.05	2.98
	II	4.73	0.00	1.60	0.04	0.02	0	0.02	0.50	2.55	7.34	5.55
Heat 4 steel + CM2 + RHA	I	1.66	0.03	0.05	0.01	0	0.01	0.11	0.01	1.44	6.23	2.57
	II	4.00	0	0.17	0.03	0	0	0	0.51	3.29	5.41	2.22
Heat 5 steel + CM3	I	4.05	0.10	0.05	1.75	0.13	1.69	0.01	0.34	0	3.36	1.79
	II	3.71	0.53	0.21	1.50	0.05	1.30	0	0.12	0	3.12	1.97
Heat 6 steel + CM3 + RHA	I	4.78	0.08	4.21	0.07	0	0.08	0.02	0.32	0	3.57	2.14
	II	4.22	0.70	0.33	1.42	0.02	1.31	0	0.44	0	4.80	6.96

3.2. Slag analysis

Tables 5 and 6 show elemental chemical composition for CM1 and CM3 slags taken from MgO crucibles after the heats, as well as solid fraction and phases for MgO saturation, using initial composition of materials (Figures 4 and 5).

Figures 6 to 8 show Al_2O_3 thermodynamic driving forces (Δc) for all the covering materials studied, without the presence

of RHA. The Δc is calculated as the difference between the red dot (circle) to the vertex of the line directed to Al_2O_3 .

Finally, Table 7 shows liquid fraction (wt. %), solid fraction (wt. %), liquid viscosity (Pa.s) and effective slag viscosity (Pa.s), for each material at the temperature of 1540 °C.

Tables 5 and 6 show elemental chemical composition variation for CM1 and CM3, considering slag samples were

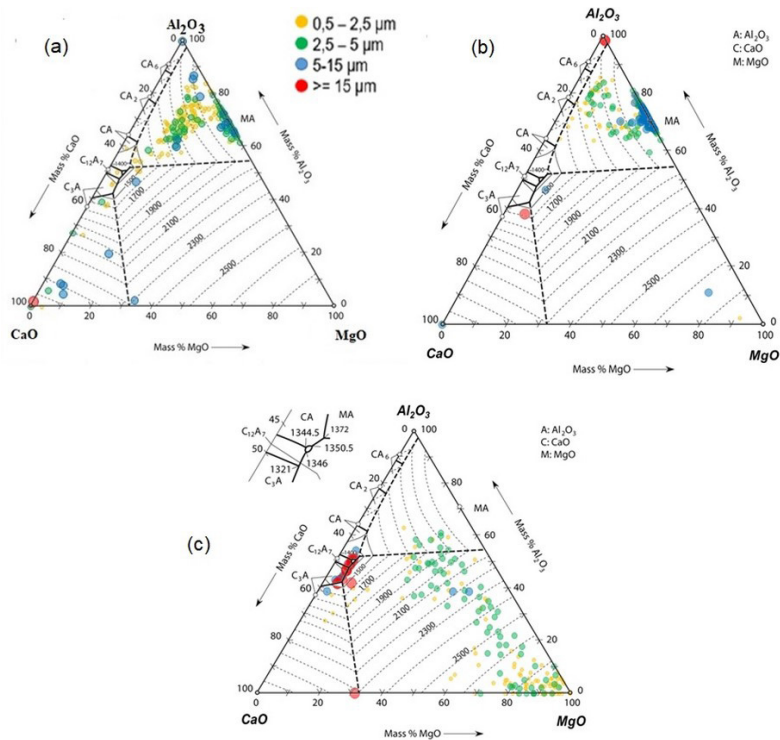


Figure 3. (a) benchmark steel sample, (b) Heat 6 Test I and (c) Heat 6 Test II.

Table 5. Elemental chemical composition for CM1 slags taken from MgO crucibles after the heats (wt%).

Arrangement	Sample	%CaO	%SiO ₂	%Al ₂ O ₃	%MgO
CM1	as-received	55.7	5.3	20.7	17.2
steel + CM1	I	48.1	9.2	23.2	18.6
	II	48.5	8.8	24.0	17.9
steel + CM1 + RHA	I	43.4	18.8	22.0	14.8
	II	39.9	18.2	18.1	13.4

Table 6. Elemental chemical composition for CM3 slags taken from MgO crucibles after the heats (wt%).

Arrangement	Sample	%CaO	%SiO ₂	%Al ₂ O ₃	%MgO
CM3	as-received	48.4	0.7	48.6	1.8
steel + CM3	I	45.5	1.0	43.2	9.4
	II	46.3	1.0	43.1	9.3
steel + CM3 + RHA	I	41.2	10.2	37.7	10.6
	II	42.3	10.0	39.6	7.8

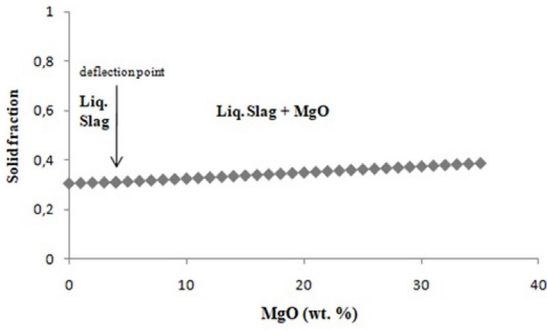


Figure 4. Solid fraction and phases encountered for MgO saturation, with initial composition for CM1.

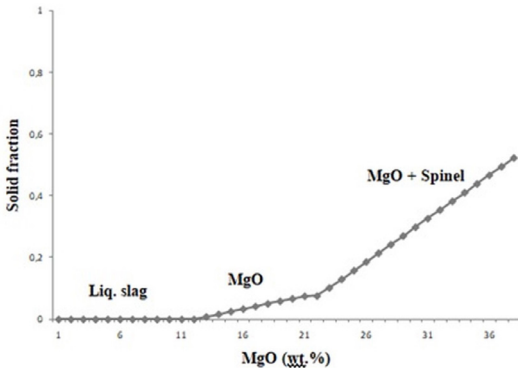


Figure 5. Solid fraction and phases encountered for MgO saturation, with initial composition for CM3.

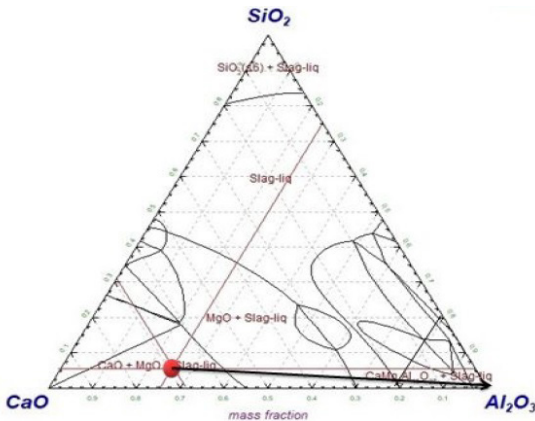


Figure 6. Al_2O_3 thermodynamic driving force (Δc) for the CM1.

collected from the same MgO crucibles used during laboratory tests. CM2 was not chosen for these tests because CM1 and CM3 showed higher differences in results, regarding mean diameter, for example. These samples (CM1 and CM3) were submitted to XRF analysis. Chemical interactions occurred among steel, tundish slag, and refractory, during the heating of 30 minutes.

Regarding Table 5, it shows that $\%SiO_2$ changed significantly for the arrangement (steel + CM1 + RHA) the

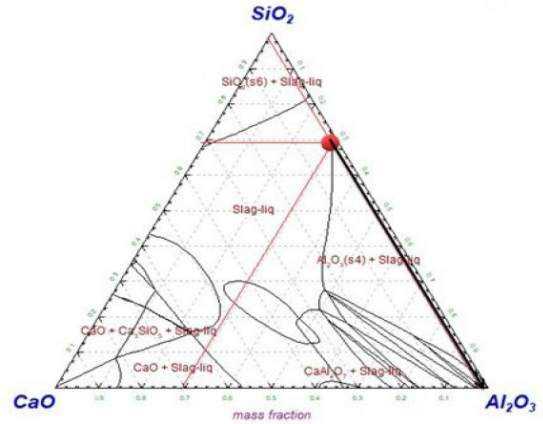


Figure 7. Al_2O_3 thermodynamic driving force (Δc) for the CM2.

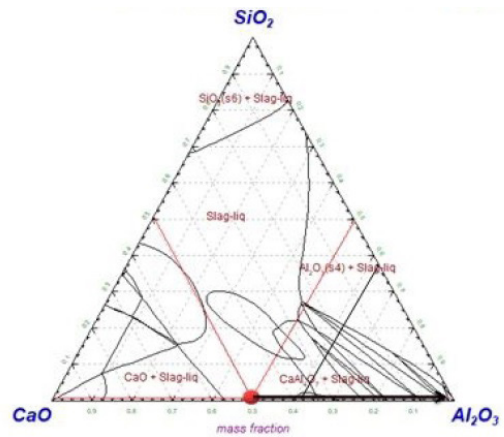


Figure 8. Al_2O_3 thermodynamic driving force (Δc) for the CM3.

content values of calcium oxide (CaO) and $\%Al_2O_3$ after the experiments presented a downward trend, while SiO_2 increased significantly mainly after the addition of RHA. This increase provides silica dissolution for the slag and can take side on liquid steel reoxidation and rising of non-metallic inclusion (NMI) particles¹³⁻¹⁵. The content of $\%MgO$ did not change significantly, except for the result of sample II with the increment of RHA. This stability can be explained by its saturation in the slag, as can it be seen on Figure 4. After simulation of MgO saturation using thermodynamic calculations (Figure 4), it can be concluded that the initial material CM1 is already saturated in this phase. According to the simulation done by *FactSage*, the first MgO solid rises after a subtle inflection around 4% in mass.

Regarding Table 6, for CM3 slags for the arrangement (steel + CM3 + RHA), the content of SiO_2 also increased significantly due to SiO_2 absorption from RHA. The content of $\%CaO$, $\%Al_2O_3$ and $\%MgO$ did not change significantly. Table 6 shows that $\%SiO_2$ also increased significantly for CM3 slags, due to SiO_2 absorption from RHA, like what happened for CM1. However, for CM3 the $\%MgO$ increased a lot for the combinations steel + CM3 and steel + CM3 + RHA. The as-received CM3 was not saturated in MgO, and

then a high amount of MgO from the crucible dissolved in the slag. According to thermodynamic calculations, the saturation point for the as-received CM3 is close to 12%, Figure 5. Close to 22% another solid complex phase rises, the spinel type.

In a previous work⁹, the composition changes of a calcium aluminate covering material (like CM3) were analyzed, comparing the as-delivered material with tundish slag samples collected at the melt shop. It was found that slag sample compositions were quite different from the composition of the as-delivered material, due to the absorption of SiO₂ from the top layer of rice husk ash.

The original composition was 58.0% CaO, 30.2% Al₂O₃, 3.3% SiO₂, and 1.5% MgO (wt%). Slag samples were collected from six heats. SiO₂ content increased, reaching high values (22.7 - 41.0%) and hence CaO e Al₂O₃ contents decreased for all the heats. With these compositional data, thermodynamic calculations were performed with the software *FactSage*. Despite the composition change, the slag remained completely liquid. Al₂O₃ activity increased from 0.01 to 0.17, which means that precipitation of Al₂O₃ solid phases was not predicted.

Thus, according to this work in literature, the ability of the slag to absorb and remove the harmful non-metallic alumina inclusions from the liquid steel was still high, even with the compositional change which happens during the continuous casting of steel.

When comparing these industrial results⁹ with the lab results of the present work, the same tendency is observed. i.e., SiO₂ from RHA was absorbed by liquid calcium-aluminate slag (steel + CM3 + RHA), changing slag composition and

increasing Al₂O₃ activity, which in turn impaired the slag's ability to absorb inclusions. Without RHA, for the setup steel + CM3, steel cleanliness is better since inclusion density and mean diameter have best values.

Table 7 shows the results obtained from thermodynamic calculations for the initial stage of each arrangement. It shows the chemical composition of CM1, presenting a liquid fraction of 65.85%, liquid viscosity of 0.118 Pa.s and effective viscosity of 0.335 Pa.s.

Viscosity values for different kinds of tundish slags were experimentally measured with rotating viscosimeter^{3,16}. It was found that the slags with high dissolution rate for Al₂O₃ and MgO.Al₂O₃ particles have low viscosity. Viscosity is an important parameter for the dissolution process, due to mass transport by diffusion and convection.

Inclusion removal is key in the production of high quality steel. The inclusions are primarily removed from liquid steel by reacting with a liquid slag phase. For efficient inclusion removal, the inclusions transfer across the steel/slag interface to dissolve in the slag. This transfer process is strongly influenced by interfacial phenomena¹⁷.

Table 8 shows the liquid phase composition of the materials studied in this work at 1540 °C, calculated in *FactSage* Equilibrium module. This data is important to allow a comparison with the results of Monaghan et al.¹⁷.

According to Monaghan et al.¹⁷, through a work of adhesion analysis it was shown that ladle type slags, with bigger relation CaO / SiO₂ + Al₂O₃, appeared more suitable for inclusion removal. In addition, that from a wetting perspective, calcium aluminate would be easier to remove than spinel and alumina. Therefore, CM1 and CM3 are

Table 7. Liquid fraction (wt. %), solid fraction (wt. %), liquid viscosity (Pa.s) and effective slag viscosity (Pa.s), for each material (T=1540 °C).

Materials	Liquid fraction (%)	Solid fraction (%)	Liquid viscosity (Pa.s)	Effective viscosity (Pa.s)
CM1	66.85	34.15	0.118	0.335
CM2	92.85	7.14	86.69	104.34
CM3	100.00	0.00	0.186	0.186

Table 8. Liquid phase composition of the materials studied in this work, in wt.%.

Materials	T start liquid phase °C	% liquid phase 1540°C	%CaO	%SiO ₂	%Al ₂ O ₃	%MgO	%FeO	%TiO ₂	%CaO / %SiO ₂ + %Al ₂ O ₃
CM1 as received	1292.48	66.85	55.04	7.92	30.8	4.84	1.2	0.15	1.42
CM2 as received	1152.05	92.85	2.26	66.6	23.17	2.15	4.5	1.28	0.03
CM3 as received	1241.98	100	48.35	0.7	48.6	1.8	0.5	0.1	0.98
RHA as received	1249.18	7.68	9.2	66.1	1.3	23.5	-	-	0.14
steel + CM1 I	NC	83.04	48.1	9.2	23.2	18.6	-	-	1.48
steel + CM1 II	NC	83.75	48.5	8.8	24	17.9	-	-	1.50
steel + CM1 + RHA I	NC	92.8	43.9	18.8	22	14.8	-	-	1.07
steel + CM1 + RHA II	NC	83.54	39.9	18.2	18.1	13.4	-	-	1.10
steel + CM3 I	NC	97.5	45.6	1	43.2	9.4	-	-	1.03
steel + CM3 II	NC	98.0	46.3	1	43.1	9.3	-	-	1.05
steel + CM3 + RHA I	NC	98.6	41.2	10.2	37.7	10.6	-	-	0.86
steel + CM3 + RHA II	NC	99.7	42.3	10.0	39.6	7.8	-	-	0.85

NC – not calculated.

more suitable for inclusion removal, but CM3 has bigger liquid fraction. Concerning the temperature of start melting, CM1 and CM3 has a difference about 50°C.

Regarding MgO saturation, the CM3 material has 1.8% MgO, which is well below the saturation content. After the tests, it was observed an incorporation of MgO in the order of 8 -10% according to Table 6. A previous addition of MgO will be beneficial in the sense of minimizing the wear of the refractory of the tundish. The refractory wear is also a function of the number of runs cast, so for smaller sequential runs the total wear will be lower.

4. Conclusions

The objective of this work is to evaluate, in laboratory, the effect of three tundish covering powders on inclusion cleanliness for a SAE 1055 modified steel - a Ca-aluminate, a Ca-Mg-aluminate, and an Al-silicate powder, analysing their interaction with rice hull ash.

The addition of RHA impairs the cleanliness of steel. The worst result, when considering inclusion density for the size > 15 µm, is from the arrangements CM1 + steel and CM1 + RHA + steel, where CM1 is a Ca-Mg-aluminate slag and RHA is rice hull ash. Otherwise, inclusion mean diameter is higher for the Ca-Mg-aluminate slag.

CM3 slag (Ca-aluminate slag), is less harmful for the steel cleanliness. The experiments with this material showed the lowest inclusion mean diameter and best capacity to absorb the impurities due to their high liquid fraction (100%). Furthermore, the driving force (Δc) for dissolution of Al_2O_3 analyzed for this material, as-received, showed a reasonable value, indicating the capacity to absorb this kind of inclusion. The material CM1 demonstrated the worst numbers considering mean inclusion diameter and slag liquid fraction (65.85%), although it had the highest driving force delta for dissolution of alumina.

Observing the results obtained, despite the interaction between the refractory material and the slag, it is possible to evaluate the effect of different compositions of covering materials on the formation / modification / removal of inclusions and the effect of the presence of calcined rice husk on inclusionary cleanliness. The methodology applied can be considered as a more severe test than the industrial conditions, but important for a pre-qualification of the covering materials of the continuous casting tundish.

5. Acknowledgments

The authors would like to thank the Ironmaking and Steelmaking Laboratory (LaSid) research team from the Federal University of Rio Grande do Sul and also CNPq and Fundação Luiz Englert for the financial support.

6. References

1. Bessho N, Yamasaki H, Fujii T, Nozaki T, Hiwasa S. Removal of inclusion from molten steel in continuous casting tundish. *ISIJ Int.* 1992;32:157-63.

2. Yang G, Wang X, Huang F, Wang W, Yin Y, Tang C. Influence of reoxidation in tundish on inclusion for Ca-treated Al-killed steel. *Steel Res.* 2014;8:784-92.
3. Holappa L, Kekkonen M, Louhenkilpi S, Hagemann R, Schröder C, Scheller P. Active tundish slag. *Steel Res.* 2013;84:638-48.
4. Neves EG, Viana JF. Application of Teccob 2504 as insulating powder and inclusion assimilation capabilities. In: 46th Steelmaking Seminar – International; 2015; Rio de Janeiro. Proceedings. São Paulo: ABM; 2015. ABM Week.
5. Aminorroaya S, Azari K, Edris H, Dippenaar R. Basic Tundish powder evaluation for continuous casting for clean steel. In: AISTech – The Iron & Steel Technology Conference and Exposition; 2006 May 1-4; Cleveland, OH. Proceedings. USA: AISTech; 2006.
6. Manninen V, Lamo T, Holappa L. Low reoxidation tundish metallurgy at Fundia Koverhar steel plant. *Scand J Metall.* 2000;29:156-65.
7. Watkinson H, Bain K, Ludlow V. A study of tundish powders and their influence on tundish slag chemistry and steel cleanliness for carbon and stainless steels. Luxembourg: European Commission; 1997. Technical Steel Research. Steelmaking. Report EUR 17845.
8. Pereira MMSM, Klug JL, Heck NC, Monteiro CC Fo, Freitas SL, Ferreira MAA, Jung D. Tundish flux practice: comparison between rice hull ash and fly-ash based tundish flux considering some relevant thermodynamic properties. In 20th IAS Steel Conference; 2014; Rosario, Santa Fe, Argentina. Proceedings. Argentina: IAS; 2014.
9. Pereira MMSM, Lima MT, Ferreira GT, Tavernier H, Klug JL, Heck NC, Jung D. Tundish slag capacity to absorb inclusions when using calcium aluminate-based covering material combined with rice hull ash. In 47th Steelmaking Seminar - International; 2016; Rio de Janeiro. Proceedings. São Paulo: ABM. ABM Week.
10. Alves PC, Da Rocha VC, Pereira JAM, Bielefeldt WV, Vilela ACF. Evaluation of thermodynamic driving force and effective viscosity of secondary steelmaking slags on the dissolution of Al_2O_3 -based inclusions from liquid steel. *ISIJ Int.* 2021;61:2092-9.
11. Bale CW, Belisle E, Chartrand P, Deckerov SA, Eriksson G, Gheribi AE, et al. FactSage thermochemical software and databases. 2010-2016. CALPHAD: Comput Coupling Ph Diagr Thermochem. 2016;54:35-53.
12. Roscoe R. The viscosity of suspensions of rigid spheres. *Br J Appl Phys.* 1952;3:267-9.
13. Alves PC, Pereira JAM, Da Rocha VC, Bielefeldt WV, Vilela ACF. Laboratorial analysis of inclusions formed by reoxidation in tundish steelmaking. *Steel Res.* 2018;89(11):1800248.
14. Da Rocha VC, Alves PC, Pereira JAM, Leal LP, Bielefeldt WV, Vilela ACF. Experimental and thermodynamic analysis of MgO saturation in the $CaO-SiO_2-Al_2O_3-MgO$ slag system melted in a laboratory resistive furnace. *J Mater Res Technol.* 2019;8(1):861-70.
15. Yan P, Arnout S, Van Ende MA, Zinngrebe E, Jones T, Blandpain B, Guo M. Steel reoxidation by gunning mass and tundish slag. *Metall Mater Trans, B, Process Metall Mater Proc Sci.* 2015;46B:1242-51.
16. Yehorov A, Ma G, Volkova O. Interaction between $MgO-C$ -bricks and ladle slag with a 1:1 CaO/Al_2O_3 ratio and varying SiO_2 content. *Ceram Int.* 2021.
17. Monaghan BJ, Abdeyazdan H, Dogan N, Rhamdhani MA, Longbottom RJ, Chapman MW. Effect of slag composition on wettability of oxide inclusions. *ISIJ Int.* 2015;55(9):1834-40.